ChemComm
Chemical Communications

This article can be cited before page numbers have been issued, to do this please use: S. Liu, S. Li, X. Shen, Y. Wang, J. Du, B. Chen, B. Han and H. Liu, *Chem. Commun.*, 2020, DOI: 10.1039/C9CC09480F.

ROYAL SOCIETY OF CHEMISTRY

rsc.li/chemcomm

View Article Online
DOI: 10.1039/C9CC09480F

Journal Name

COMMUNICATION

Selective aerobic oxidation of cyclic ethers to lactones over Au/CeO_2 without any additives

Received 00th January 20xx,
Accepted 00th January 20xx

DOI: 10.1039/x0xx00000x

www.rsc.org/

Shulin Liu[a,b], Shaopeng Li[a,b], Xiaojun Shen[a,b], Yanyan Wang[a,b], Juan Du[a,b], Bingfeng Chen*[a], Buxing Han[a,b] and Huizhen Liu* [a,b]

Selective oxidation of ethers to lactones with O_2 as benign oxidant using Au/CeO_2 as the catalyst has been developed. The oxygen vacancies and Au^0 species on the surface of CeO_2 contribute to the activation of O_2. The excellent selectivity of lactones is due to the adsorption of ethers and activation of C(sp^3)-H bond on Au/CeO_2.

The oxidation of cyclic ethers to lactones is of paramount importance in synthetic organic chemistry and industry of fine chemicals because of their use in a wide range of products, such as perfumers, pharmaceutical intermediates, and industrial solvents for polymer polymerization, etc.[1-3] The conversion routes have been developed using stoichiometric oxidants such as $NaIO_4$, $KMnO_4$ or H_3PO_4, which generate enormous amounts of waste.[4-8] For example, Gong group reported the oxidation of tetrahydrofuran (THF) using equivalent $NaIO_4$ as the oxidation agent over iridium–bipyridine complexes IrCp-BPy-NT derived from bipyridine-based organosilica nanotubes.[9] To develop a more environmentally benign oxidation systems, the processes of using H_2O_2 as an oxidant on heterogeneous catalyst were also reported.[10-11] For instance, Sooknoi et al. reported the heterogeneous process of using H_2O_2 as an oxidant on iron-containing clay catalyst, and the yield and the selectivity of γ-butyrolactone (GBL) was 16.65% and 61.87%, respectively.[10]

Molecular oxygen (O_2) is the most ideal oxidant[12] for oxidation reaction because of its green and clean characteristics. Due to the increasing environmental concerns, many efforts have been devoted to develop the oxidation systems using O_2 as the oxidant. The selective aerobic oxidation of THF to GBL using a homogeneous iron complex catalyst has been reported.[13] Wu group developed a catalyst CZJ-22-Cu by suspending ionic single atoms (ISAs) inside the anionic pores of metal–organic frameworks (MOFs), exhibited high catalytic efficiency in oxidation of ethers to esters with O_2 as an oxidant in the presence of NHPI.[14] Carbon dioxide mediated aerobic oxidation of ethers catalysed by rhodium-based catalyst have also been reported.[15] It is obviously that the catalytic systems which have been reported for the oxidation of cyclic ethers using O_2 as the oxidant have some shortcomings, such as complicated catalyst synthesis methods, high cost, toxicity, pollution and so on because of the usage of the homogeneous catalyst or additives. It is highly desirable to develop a heterogeneous catalytic system using O_2 as the oxidant without any additives. However, it is a great challenge because of the inertness of C(sp^3)-H bond.[16-19]

CeO_2-supported catalysts have been extensively studied in the oxidation reaction because it possesses outstanding oxygen storage and release capacities.[20-23] In this work, we developed a heterogeneous catalytic system Au/CeO_2 for the selective aerobic oxidation of cyclic ethers to lactones in the absence of any additives for the first time. The yield and selectivity of γ-butyrolactone (GBL) for the selective oxidation of tetrahydrofuran (THF) could be 15.4% and 91.3%, respectively. A possible free radical reaction mechanism was proposed, in which the activation of C(sp^3)-H bond may be the rate-determining step of the reaction.

The CeO_2 support was prepared via the modified hydrothermal method with cerium nitrate hexahydrate as the precursor (See from supporting information).[24] The Au/CeO_2 catalyst was prepared by impregnation method. The transmission electron microscopy (TEM) images of CeO_2 and Au/CeO_2 are shown in Fig. 1. The CeO_2 support exhibits a shape of nanorod (length:90-150 nm) with a diameter ranging from 10 to 20 nm before and after Au deposition (Fig. 1A and 1B). The TEM images of Au/CeO_2 is shown in Fig. 1B, the Au nanoparticles were dispersed uniformly on the CeO_2 nanorods with an average diameter of 3.19±0.08 nm (Fig. 1D), indicating that the Au/CeO_2 catalyst was obtained successfully. The loading content of Au is 2.16 wt% analyzed by inductively coupled plasma (ICP) mass spectrometry.

X-ray diffraction spectra (XRD) analysis was carried on to investigate phase structure of the catalysts, and the results are shown in Fig. 1C. The diffraction peaks of the prepared catalysts could be indexed to the pure fluorite cubic structures (JCPDS No. 34-0394), indicating that the CeO_2 in cubic phase was synthesized.[24] A small diffraction peak of metallic Au (JCPDS No. 04-0784) species was

---

[a] *Beijing National Laboratory for Molecular Sciences, CAS Key Laboratory of Colloid and Interface and Thermodynamics Institute of Chemistry, Chinese Academy of Sciences, Beijing 100190,P. R. China. Email: chenbf@iccas.ac.cn, liuhz@iccas.ac.cn*
[b] *University of Chinese Academy of Sciences, Beijing 100149, P. R. China.*

Electronic Supplementary Information (ESI) available: Experimental procedure and additional figures. See DOI: 10.1039/x0xx00000x observed in Au/CeO_2 patterns, indicating the high dispersion of Au species.

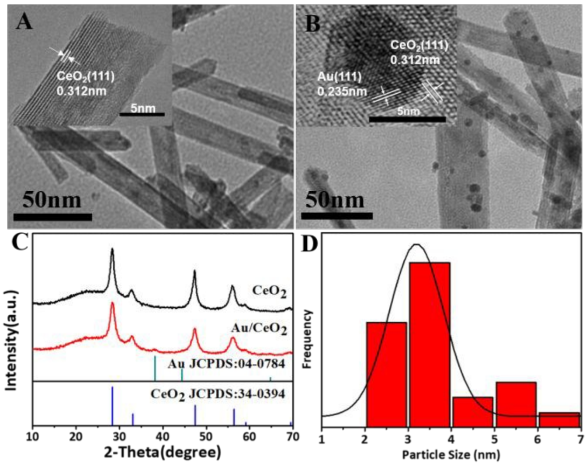

Fig.1 TEM images of CeO_2 (A), Au/CeO_2 (B), XRD patterns of CeO_2 and Au/CeO_2 (C) and particle size distribution histogram (D).

Table 1 Catalytic performance of controlled experiment [a]

Entry	Catal.	Conv. (%)	Yield[b] (%)		Selectivity[c] (%)	
			GBL	Propylformate	GBL	Propylformate
1	--	47.8	6.6	7.2	25.9	33.0
2	CeO_2	45.3	7.3	8.5	20.1	31.8
3	Au/CeO_2	41.2	13.7	0.5	90.5	2.1
4[d]	Au/CeO_2	46.0	15.4	0.5	91.3	1.6

[a] Reaction conditions: THF (2 mL), catalyst (20 mg), T (100°C), t (6 h), PO_2(1 MPa) and stirring speed (600 rpm). [b] Yields of GBL and propylformate were determined by GC with n-decane as internal standard. [c] Selectivity based on the peak area of all the products detected. [d] The temperature is 120°C.

The performance of the catalyst was evaluated using the oxidation of THF as the model reaction. GBL and propylformate were the main products. In the absence of any catalyst, the yield and the selectivity of GBL was only 6.6% and 25.9% (Table 1, entry 1), respectively. The yield of GBL increased to 7.3% over CeO_2, while the selectivity was only 20.1% (Table 1, entry 2). CeO_2 improved the yield of GBL. However, the increase of GBL yield was accompanied by the increase of the yield of other by-products, which led to a slight decrease in the selectivity of GBL compared with that without catalyst. Au/CeO_2 showed better catalytic performance in the reaction. The yield of GBL could reach 13.7% and the selectivity increased to 90.5% accompanied with minor amount of propylformate (yield: 0.5%) (Table 1, entry 3). When the temperature increased to 120 °C, the GBL increased to 15.4% (Table 1, entry 4). Interestingly, in the presence of CeO_2 and Au/CeO_2, the conversion of THF decreased slightly, which may be due to the change of reaction path by the catalyst. The reaction mechanism will be discussed below.

The effect of temperature on the efficiency of the reaction was firstly checked in the absence of any catalyst (Fig. S1). The yield of GBL was very low at 40°C to 80°C. At 100°C, the yield of GBL increased to 6.6%. However, the higher temperature leads to the cleavage of C-C skeleton to form propylformate with 7.2% yield. The effect of reaction temperature was also studied over Au/CeO_2 (Fig. 2A). At 60°C, the yield of GBL was also very low on Au/CeO_2. The

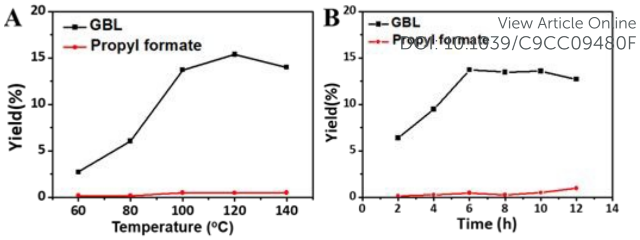

View Article Online
DOI: 10.1039/C9CC09480F

Fig. 2 Temperature curve in 6 h (A) and time curve under 100 ℃ (B) with Au/CeO_2 catalyst. Reaction conditions: THF (2 mL), catalyst (20 mg), PO_2 (1 MPa), and stirring speed (600 rpm). Yields of GBL and propylformate were determined by GC with n-decane as internal standard.

GBL yield increased greatly with increasing temperature (from 60 ºC to 100 ºC), and the yield of propylformate decreased. At 100°C, the yield of GBL was 13.7% and increased to 15.4% at 120°C. However, further elevating temperature resulted in decrease of GBL yield. So, the optimized reaction temperature was 120°C. Compared with the reaction in the absence of catalyst, Au/CeO_2 enhanced the selectivity of GBL and inhibited by-products formation. The selectivities of GBL and propylformate were 91.3% and 1.6% at 120 °C (Fig. S2D), respectively. Fig. 2B presented the influence of time on the yield of GBL at 100°C. The yield of GBL increased in the initial stage of the reaction until 6 h. Subsequently, the yield decreased slightly because more propylformate was produced with the prolongation of reaction time. This result may be resulted from over-oxidation with the reaction time extending.

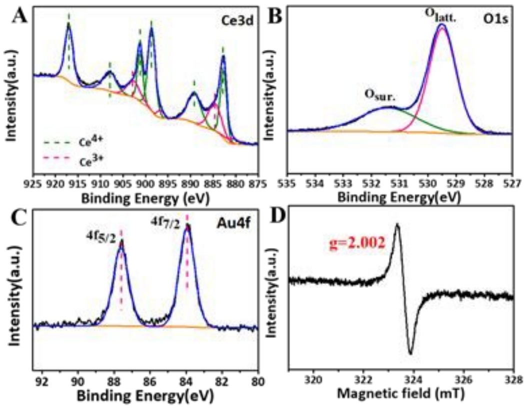

Fig. 3 XPS spectrum of Ce 3d (A), Au 4f (B), O1s (C) and EPR spectra (D) of Au/CeO_2 nanorods.

XPS spectra were employed to probe the chemical states of the Au species and surface cerium species in Au/CeO_2 catalyst. For the Ce 3d spectra as shown in Fig. 3A, eight peaks resulting from the pairs of spin orbit doubles can be identified through deconvolution method, according to the previous reports.[25] Six peaks located at 900.3 eV, 906.9 eV, 916.1 eV, 881.9 eV, 888.5 eV and 897.6 eV are characteristic of Ce^{4+}. While the other two peaks located at 883.9 and 901.9 eV could be assigned to Ce^{3+}, which is often used as an indicator for the existence of oxygen vacancies (OVs) on ceria surface.[26] Furthermore, there can be fitted with two peaks in the O1s spectrum (Fig. 3B). One peak at 529.4eV is attributed to crystal lattice oxygen bonded with Ce^{4+} to form Ce-O bond. The other is assigned to the chemisorbed O on CeO_2 surface. In addition, the EPR spectra,

View Article Online
DOI: 10.1039/C9CC09861E

as shown in Fig. 3D, presents a peak with a g value of 2.002, [27] also suggesting the formation of OVs due to the Ce^{3+} in the CeO_2, which is consisted with the results of Ce 3d XPS analysis. OVs on CeO_2 could promote the adsorption of O_2 and make it easier for zero-valent metal species to interact with O_2.[28-29] Electrons transfer from zero-valent metal species to π* orbitals of oxygen molecules to activate O_2.[29] Fig. 3C presents the Au 4f XPS spectra of the gold catalyst. The spin-orbit split peaks located at 83.93eV and 87.55eV are ascribed to Au^0 species.[30-31] Au^0 species on the support play a vital important role in O_2 activation and lead to an efficient catalytic activity in the selective aerobic oxidation of THF. The reusability of Au/CeO_2 was tested for the oxidation of THF to GBL. Unfortunately, the yield and selectivity of GBL decreased from 13.7% to 7.0% and 90.5% to 54.1%, respectively. The deactivation of the catalyst attributed to the agglomeration of Au nanoparticles as the TEM image shows (Fig. S4).

To study the reaction mechanism, some control experimens were performed. The aerobic oxidation of THF over Au/CeO_2 was almost fully suppressed after addition of free radical scavenger, butylated hydroxytoluene (BHT). It has previously reported that BHT suppresses the formation of superoxide radical anion ($\cdot O^{2-}$).[32] These results demonstrate that the reaction proceeded through a free radical mechanism.

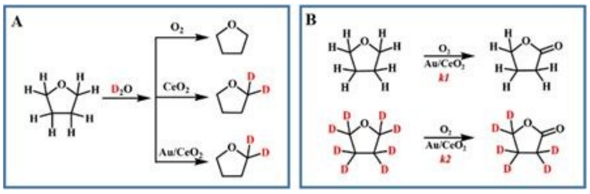

Scheme 2 H-D exchange (A) and deuterium dynamics experiments (B).

Table 2 Isotope abundance of m/z 71, 72, 73 in THF in H-D exchange experiment [a]

Entry	Reaction	Isotope Abundance [d] (%)		
		71	72	73
1[b]	——	45.21	33.33	21.46
2[c]	O_2	45.32	31.87	22.81
3	CeO_2	43.85	32.31	23.85
4	Au/CeO_2	43.30	30.31	26.39

[a] Reaction conditions: THF (2 mL), D_2O (10 mmol), catalyst (20 mg), T (100°C), t (6 h), and stirring speed (600 rpm). [b] without D_2O, [c] PO_2 (1MPa). [d] Isotope abundance of m/z was determined by GC-MS.

The activation of $C(sp^3)$-H bond is the key step in the oxidation of THF. Therefore, a H-D exchange experiment was carried out in the presence of D_2O to observe how the $C(sp^3)$-H bond was activated in the catalytic process (Scheme 2A). As shown in Table S1, the isotope abundance (Fig. S3) of THF at m/z of 73 is 21.46% and it increased slightly to 22.81% in O_2 atmosphere without catalyst (Table 2, entry 1 and 2). However, it increased to 26.39 % in the presence of Au/CeO_2 (Table 2, entry 4) which means that H atoms of partial THF are replaced by D atoms with D_2O, and this exchange is likely to occur on the α-hydrogen of THF.[33] This result indicates that Au/CeO_2 could activate the $C(sp^3)$-H bond of THF. CeO_2 also could activate the $C(sp^3)$-H bond of THF and the isotope abundance at m/z of 73 increased to 23.85% (Table 2, entry 3). Obviously, the activity of Au/CeO_2 for the activation of $C(sp^3)$-H bond is higher than CeO_2, which is consistent with the activity for the selective aerobic oxidation of THF (Table 1, entries 2 and 3). These results show that the activation of $C(sp^3)$-H bond is critical. In addition, in a typical kinetic experiments (Scheme 2B), the ratio of reaction rate constant of THF and THF-D8 was 2.04 ($k_H/k_D = 2.04$), within the range of the second kinetic isotope effect (SKIE), illustrated that the activation of C-H bond was the rate-determining step in the aerobic oxidation of THF.

From the GC spectrum of liquid mixture was shown in Figure S2, it is obviously that the main product was GBL and propylformate for the THF oxidation. More propylformate was formed in the absence of Au/CeO_2 catalyst. It is well known that ethers are easy to form hydroperoxides on exposure to oxygen, especially in high temperature.[34] According to the experimental results and the chemical knowledge in the literature,[34-37] the reaction pathway was proposed to occur via a β-scission of an alkoxy radical (Scheme 3 path a).

A possible reaction pathway to form lactones was also proposed as follows based on above results and supported by previous studies (Scheme 3 path b).[38-40] Firstly, the adsorption of oxygen on support is enhanced by the presence of oxygen vacancies on the surface of CeO_2, which makes it easier for electron transfer from Au^0 species to O_2, thus generate the superoxide radicals ($\cdot O^{2-}$). At the same time, THF was adsorbed on the interface between Au NPs and CeO_2 support and the C-Ha/Hb was activated. Subsequently, the activated C-Ha bond was attacked by superoxide radicals to form 2-hydroperoxytetrahydrofuran intermediate. Finally, the desired product GBL was obtained accompanied by a molecular H_2O removed in a catalytic cycle. From above preliminary mechanism, the Au/CeO_2 nanorods catalyst inhibits the formation of alkoxy radicals by adsorbing THF and activating C-H bond at the interface of Au NPs and CeO_2, thus giving a rise to the selectivity in a new reaction pathway.

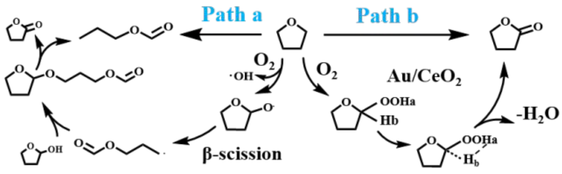

Scheme 3 Possible reaction mechanism of selective aerobic oxidation of THF over Au/CeO_2 catalyst and propylformate in the absence of catalyst.

Finally, the substrate scope of this reaction was further investigated and the related results were summarized in Table 3 and Table S1. The Au/CeO_2 catalytic system could oxidize various cyclic ethers into corresponding lactones. The yield and selectivity of γ-valerolactone and δ-valerolactone obtained from the oxidation of 2-methyltetrahydrofuran and tetrahydropyran was 9.0%， 27.3% and 2.2%， 70.0% (Table 3, entry 2 and entry 5 and Table S1), respectively. Phthalan could be oxidized with a 26.2% total yield and 94.7% selectivity (Table 3, entry 3 and Table S1). The oxidation of isochroman to produe isochromanone with 49.3% yield and 91.8% selectivity (Table 3, entry 4 Table S1). These results demonstrate that

View Article Online
DOI: 10.1039/C9CC09480F

the reactivities of aromatic ethers are higher than other aliphatic cyclic ethers in the aerobic oxidation.

In conclusion, the heterogeneous catalyst Au/CeO_2 could catalyze the selective catalytic oxidation of THF to GBL with O_2 as oxidant without any additives. Although the yields remain to be improved, a satisfactory selectivity of GBL in 91.3 % has been achieved. Preliminary mechanism studies showed that the oxygen vacancies and Au on the surface of CeO_2 contributed to the generation of superoxide radicals and the interface between Au nanoparticles and CeO_2 support could adsorb THF and further activate C(sp^3)-H bond, thus achieving high selectivity of the desired product GBL. The Au/CeO_2 catalyst is also efficiently for selective oxidation of other cyclic ethers into corresponding lactones. This work may provide helpful insights into the design of the heterogeneous catalyst for selective oxidation of other important oxygen-containing compounds.

Table 3 Au/CeO_2-catalyzed aerobic C-H oxidation of different ether substrates [a]

Entry	Substrate	Product	Yield[b](%)
1		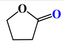	13.7%
2	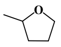	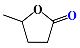	9.0%
3	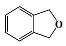	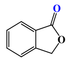	26.2%
4	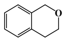	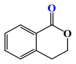	49.3%
5		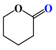	2.2%

[a] Reaction conditions: substrate (2 mL), catalyst (20 mg), T (100℃), t (6 h), PO_2(1MPa) and stirring speed (600 rpm). [b] Yield of product was determined by GC with n-decane as internal standard.

Acknowledgements

This work was supported by the National Key Research and Development Program of China (2018YFB0605801), Beijing Municipal Science & Technology Commission (Z181100004218004), National Natural Science Foundation of China (21871277). Chinese Academy of Sciences (QYZDY-SSW-SLH013).

Notes and references

1 A. Miyafuji and T. Katsuki, *Tetrahedron*, 1998, **54**, 10339-10348.
2 J. Zhou, C. L. Fu and S. M. Ma, *Nat. Commun.*, 2018, **9**, 1654.
3 X. Y. Zhang, M. Fevre, G. O. Jones and R. M. Waymouth, *Chem. Rev.*, 2018, **118**, 839-885.
4 S. Ma, *J. Chem. Rev.*, 1998, **9**, 592-593.
5 M. T. Reezt and K. Tollner, *Tetrahedron Lett.*, 1995, **36**, 9461-9465.
6 M. Salavati-Niasari and M. Bazarganipour, *Inorg. Chem. Commu.*, 2006, **9**, 332-336.
7 Y. Ogata, K. Tomizawa and T. Ikeda, *J. Org. Chem.*, 1980, **45**, 1320-1322.
8 A. Shaabani and D. G. Lee, *Tetrahedron Lett.*, 2001, **42**, 5833-5836.
9 S. B. Zhang, H. Wang, M. Li, J. Y. Han, X. Liu and J. L. Gong, *Chem. Sci.*, 2017, **8**, 4489-4496.
10 A. Ausavasukhi and T. Sooknoi, *Green Chem.*, 2015, **17**, 435-441.
11 M. Sasidharan and A. Bhaumik, *J. Molecular Catal. A*, 2011, **338**, 105-110.
12 F. T. Du and J. X. Ji, *Chem. Sci.*, 2012, **3**, 460-465.
13 A. Gonzalez-de-Castro, C. M. Rbertson and J. L. Xiao, *J. Am. Chem. Soc.*, 2014, **136**, 8350-8360.
14 W. L. He, X. L. Yang, M. Zhao and C. D. Wu, *J. Catal.*, 2018, **358**, 43-49.
15 A. K. Fazlur-Rahman, J. C. Tsai and K. M. Nicholas, *J. Chem. Soc., Chem. Commun.*, 1992, **18**, 1334-1335.
16 Z. P. Li, R. Yu and H. J. Li, *Angew. Chem. Int. Ed.*, 2008, **47**, 7497-7500.
17 T. Newhouse and P. S. Baran, *Angew. Chem. Int. Ed.*, 2011, **50**, 3362-3374.
18 L. Ackermann, J. Pospech, *Org. Lett.*, 2011, **13**, 4153-4155.
19 A. R. Dick, K. L. Hull and M. S. Sanford, *J. Am. Chem. Soc.*, 2004, **126**, 2300-2301.
20 J. Paier, C. Penschke and J. Sauer, *Chem Rev.*, 2013, **113**, 3949-3985.
21 Y. J. Lee, G. H. He, A. J. Akey, R. Si, M. Flytzani-Stephanopoulos and I. P. Herman, *J. Am. Chem. Soc.*, 2011, **133**, 12952-12955.
22 T. Montini, M. Melchionna, M. Monai and P. Fornasiero, *Chem. Rev.*, 2016, **116**, 5987-6041.
23 D. Devaiah, L. H. Reddy, S. E. Park and B. M. Reddy, *Catal. Rev.*, 2018, **60**, 177-277.
24 X. G. Liu, K. B. Zhou, L. Wang, B. Y. Wang and Y. D. Li, *J. Am. Chem. Soc.*, 2009, **131**, 3140-3141.
25 H. L. Jia, A. X. Du, H. Zhang, J. H. Yang, R. B. Jiang, J. F. Wang and C. Y. Zhang, *J. Am. Chem. Soc.*, 2019, **141**, 5083-5086.
26 D. Damma, T. Boningari and P. G. Smirniotis, *Molecular Catal.*, 2018, **451**, 20-32.
27 J. W. Wan, W. X. Chen, C. Y. Jia, L. R. Zheng, J. C. Dong, X. S. Zheng, Y. Wang, W. S. Yan, C. Chen, Q. Peng, D.S. Wang and Y. D. Li, *Adv. Mater.*, 2018, **30**, 1705369.
28 A. Corma, P. Concepcion, M. Boronat, M. J. Sabater, J. Navas, M. J. Yacaman, E. Larios, A. Posadas, M. A. Lopez-Quitela, D. Buceta, E. Mendoza, G. Guilera and A. Mayoral, *Nat. Chem.*, 2013, **5**, 775-781.
29 H. Y. Tan, J.Wang, S. Z. Yu and K. B. Zhou, *Environ. Sci. Technol.*, 2015, **49**, 8675-8682.
30 S. L. Chen, L. F. Luo, Z. Q. Jiang and W. X. Huang, *ACS. Catal.*, 2015, **5**, 1653-1662.
31 Q. Q. Li, H. Y. Wang, Z. P. Tian, Y. J. Weng, C. J. Wang, J. R. Ma, C. F. Zhu, W. Z. Li, Q. Y. Liu and L. L. Ma, *Catal. Sci. Technol.*, 2019, **9**, 1570-1580.
32 X. J. Cui, Y. H. Li, S. Bachmann, M. Scalone, A. E. Surkus, K. Junge, C. Topf, M. Beller, *J. Am. Chem. Soc.*, 2015, **137**, 10652-10658.
33 M. Salavati-Niasari, *Inorg. Chem. Commun.*, 2006, **9**, 628-633.
34 M. Sommovigo and H. Alper, *J. Molecular Catal.*, 1994, **88**, 151-158.
35 M. Murakami and N. Ishida, *Chem. Lett.*, 2017, **46**, 1692-1700.
36 J. Setsune, Y. Ishimaru, T. Moriyama and T. Kitao, *J. Chem. Soc., Chem. Commun.*, 1991, **8**, 556-557.
37 P. Li and H. Alper, *J. Molecular Catal.*, 1992, **72**, 143-152.
38 H. Wei, and E. K. Wang, *Chem. Soc. Rev.*, 2013, **42**, 6060-6093.
39 T. Straub and A. M. P. Koskinen, *Inorg. Chem. Commun.*, 2002, **5**, 1052-1055.
40 K. Wu, L. D. Sun and C. H. Yan, *Adv. Energy Mater.*, 2016, **6**, 1600501.

View Article Online
DOI: 10.1039/C9CC09480F

For Graphical Abstract Use Only